



Suppression of photo-induced effects in chemically stoichiometric $\text{Ge}_{26.67}\text{Ga}_8\text{S}_{65.33}$ glasses

YUANHUAN SUN,¹ ZHENG ZHANG,¹ ZHEN YANG,¹ LEI NIU,¹ JIAN WU,¹ TENGXIU WEI,¹ KUNLUN YAN,² YAN SHENG,¹ XUNSI WANG,¹ AND RONGPING WANG^{1,*} 

¹The Research Institute of Advanced Technologies, Ningbo University, Ningbo 315211, China

²Laser Physics Centre, Research School of Physics and Engineering, The Australian National University, Canberra, ACT 0200, Australia

*Corresponding author: wangrongping@nbu.edu.cn

Abstract: We have prepared $\text{Ge}_x\text{Ga}_8\text{S}_{92-x}$ glasses with $x=20, 26.67$ and 36 , and investigated the photoinduced effects under illumination at sub-bandgap wavelength with different power densities. It was found that, Ge_{20} and Ge_{36} undergo photodarkening (PD) and photobleaching (PB), respectively, and the change of transmission ratio with and without illumination increases with increasing illumination power density as well as prolonging illumination time. On the other hand, $\text{Ge}_{26.67}$ is almost optical stable in any cases. This potentially offers a chance to reduce additional optical loss induced by PD and achieve net optical gain in the erbium doped chalcogenide planar waveguide amplifier using chemically stoichiometric $\text{Ge}_{26.67}$ glass.

© 2021 Optical Society of America under the terms of the [OSA Open Access Publishing Agreement](#)

1. Introduction

Chalcogenide glasses are useful in various photonic devices in the infrared because of their high linear and nonlinear refractive index, broad transmission range, ultrafast nonlinear response and low phonon energy [1–4]. Especially, low phonon energy makes rare earth ions-doped chalcogenide glasses promising to emit or amplify the light for various active applications in the infrared, since the radiative emission quantum efficiency of rare-earth ions dissolved in the glass matrix can be significantly enhanced [5,6]. For this reasons, rare earth ion-doped chalcogenide glasses have been extensively investigated as a solution available to develop new lasers working at the mid-infrared [3–7].

However, dissolving high content rare earth ions into chalcogenide is challenging since the rare earth ion clusters can be easily formed in the glasses and thus photoluminescence can be readily quenched. For example, typical As_2S_3 glasses only can host 0.1%mol Er [4,5]. One of the solutions is to add metal Ga into glass matrix, since Ga can be well dispersed in the glasses and the formation of the chemical bonds between Ga and rare earth ions can effectively reduce the number of the rare earth ion clusters [8,9]. Therefore Ga-contained chalcogenide glasses are considered as an effective medium to host rare earth ions.

Nevertheless, in the last few decades, only few successful reports on active applications from rare earth ion-doped glasses can be found in the literatures, and the lasing wavelength is mostly limited to the near infrared [10–14], but recently extended to 5-6 μm [15–16]. While lots of effects have been paid to purify Ga-contained glasses in order to decrease the defects in the glasses and thus reduce the radiation recombination, we realize that, the nature of weak chemical bonds in chalcogenide glasses compared with those in SiO_2 glasses leads to strong photo-induced effects, and their impact on active applications like optical amplifier and lasing has seldom been investigated. As mentioned above, while Ga-contained chalcogenide glasses are considered as an effective medium to host rare earth ions, we found that, optical loss can be significantly increased

at a short time scale (up to tens of seconds) when Er^{3+} doped chalcogenide waveguides were exposed to laser, and could be recovered with prolonged illumination [17]. This is clearly due to photo-induced effects in the chalcogenide glasses.

The most observable photo-induced effects in chalcogenide glasses are photodarkening (PD) and photobleaching (PB). PB represents the shift of optical transmission edge to higher energy (blue shift), and a corresponding decrease in absorption coefficient with the increase in optical bandgap E_g . PD is opposite to PB with a red shift of the optical transmission edge upon illumination. [4,18]. While their origin is still arguable, alternative explanations are from photo-induced structural change from homopolar to heteropolar bonds triggered by external energy input or photo-oxidation [19,20]. Many studies also show that chemical composition plays a decisive role in the photo-induced effects. For example, Calvez et.al. showed that PD and photo- "expansive broad band" ion tend to vanish in $\text{Ge}_x\text{As}_x\text{Se}_{1-2x}$ glasses [21]. Yang et al. [22], Su et al. [23], and Nemeč et al. [24], have independently demonstrated a photo-stable phase in Ge-As-Se films with very distinct compositions. All these indicate that, the photosensitivity can be tuned by varying the composition in Ge-As-Se ternary system [25]. However, there are no reports on Ge-Ga-S system which is very useful as the host material for rare earth ion doping. Therefore, the results in Ge-As-Se glasses inspire us to investigate the dependence of photo-induced effects on the compositions in Ge-Ga-S system.

In the present paper, we prepared Ge-Ga-S glasses with various compositions that were S-poor, chemically stoichiometric and S-rich, and investigated the transmittance with and without illumination using sub-bandgap wavelength at different power densities to understand the photo-induced effects in Ge-Ga-S glasses. The time-varying exponential function was used to model the dynamic process of photo-induced effects. The results demonstrated the possibility of tuning photo-induced effects via glass compositions, and potential decrease of optical losses in the materials via suppression of photo-induced effects could open up the avenue of the use of Ge-Ga-S glasses in various active applications.

2. Experiments

Ge-Ga-S glasses were prepared by the melt-quenching method. High pure Ge, Ga, S elements (5 N) were weighted and introduced into cleaned quartz glass ampule before the ampule was evacuated to $\sim 10^{-3}$ Pa and sealed. The ampoules were then placed in a rocking furnace, the mixture was melted at 950 °C for 12 hours, and then quenched in cold water. Then, the glass rod was annealed at 300 °C for 4 hours, and then cut into glass disks ($\varnothing 10$ mm \times 1 mm). The glass disks were further mechanically polished into a thickness of tens of micrometers.

X-ray diffraction measurements showed that, all the XRD patterns of the glasses exhibit broad bands and no any sharp peaks can be detected, confirming amorphous nature of the glasses. The chemical compositions of the glasses were determined by an energy dispersive X-ray spectrometer installed in a Tescan VEGA3 scanning electron microscope, and the difference from their respective nominal composition is less than 0.3%. Some parameters of the physical properties of the glasses can be found in Ref.(26).

We used the pump-probe method to study the photo-induced effects in these samples. The schematic diagram of the experimental set-up is shown in Fig. 1. In short, we choose high-power collimated light-emitting diodes (LED) with a central wavelength of 830 nm (1.49 eV) and a beam diameter of 5 mm. The illumination power is adjusted by a filter in front of the sample. The detection beam is low intensity white light with a diameter of 2 mm and a wavelength range of 550–1000 nm. High resolution optical absorption spectrometer (Ocean Optics HR2000) was used to record the transmittance changes before and after the pump beam irradiation at 10 ms intervals, and all the measurements were performed in air.

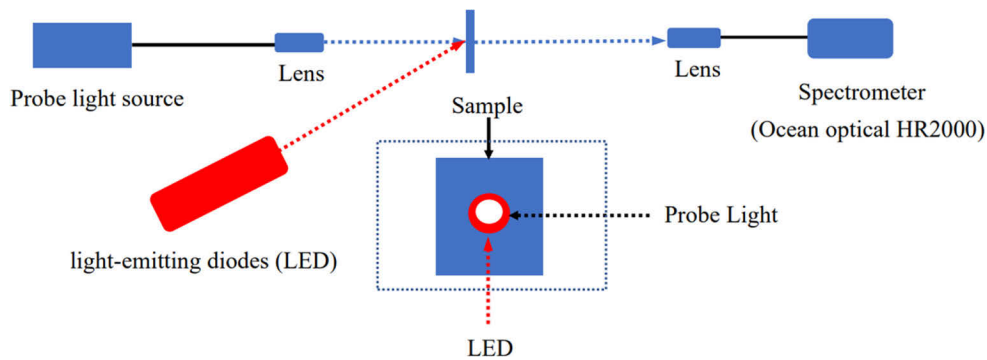


Fig. 1. Schematic diagram of the experimental set-up. The frame indicates the distribution of the illumination (red) and probe light (white) beam on the surface of the sample where the probe light beam is overlapped with the illumination beam, but the former one is less than the latter one in the size of the beam as stated in the text.

3. Results and discussion

Regarding photo-induced effects, the difference in as-prepared, annealed films and bulk glasses in terms of quasi-stability and structural disorder have been emphasized [4,18]. The annealed films and bulks have the lowest free energy and smallest disorder, and photo-excitation always produces more unstable and more disordered states, therefore photo-induced effects in the annealed films and bulks are reversible. On the other hand, the as-prepared films are likely to be energetically higher or lower than the illuminated state, therefore, illumination effects become irreversible [4]. Irreversible or Reversible change are defined as whether photo-induced effects can be erased by thermal annealing at some temperatures. In the present paper, thin bulk glasses were used to investigate photo-induced effects in Ge-Ga-S system.

On the other hand, if Ga content is fixed at 8%, the chemically stoichiometric composition is $\text{Ge}_{26.67}\text{Ga}_8\text{S}_{65.33}$, considering that Ge, Ga and S is four-, three- and two-coordinated, respectively, in the glasses [26]. In the present experiments, we measured photo-induced effects in the glasses with various compositions and we found three different behaviors in the glasses corresponding to three different compositional range, e.g., S-rich, chemically stoichiometric and S-poor, respectively. Therefore we only report the typical results here. The LED with four different power density of 10, 122, 244, 400 mW/cm^2 were used to illuminate the samples with an illumination time up to 10000 s. Below are the details of the experimental results.

The transmission spectra of as-prepared and illuminated samples were measured and the results were shown in Figs. 2(a), 1(b) and 1(c) for Ge_{20} ($\text{Ge}_{20}\text{Ga}_8\text{S}_{72}$), $\text{Ge}_{26.67}$ ($\text{Ge}_{26.67}\text{Ga}_8\text{S}_{65.33}$) and Ge_{36} ($\text{Ge}_{36}\text{Ga}_8\text{S}_{56}$), respectively. It is clear seen that, the transmission edge of the illuminated sample has a significant red shift (moving to longer wavelength) compared with the as-prepared sample in Fig. 1(a) for Ge_{20} , while the dash shifted (moves to shorter wavelength) for Ge_{36} in Fig. 1(c), and it seems no change upon illumination for chemically stoichiometric $\text{Ge}_{26.67}$ sample as shown in Fig. (b).

We used the Tauc plots to determine the optical band gap of these samples in the as-prepared and illuminated states under different power densities of 10, 122, 244, and 400 mW/cm^2 , respectively. After the samples were illuminated under a power density of 400 mW/cm^2 , they were annealed at a temperature that was 20°C lower than their respective glass transition temperature (following the data in Ref.(26)) for 2h, and their optical band gaps were also measured using the same method. All the results are listed in Table 1. From the change of the optical band gap, we can conclude that for Ge_{20} sample, the energy of the optical band gap decreases from 2.45 eV to 2.4 eV, but this is reversible to 2.45 eV with further annealing, and thus this is a PD process. However,

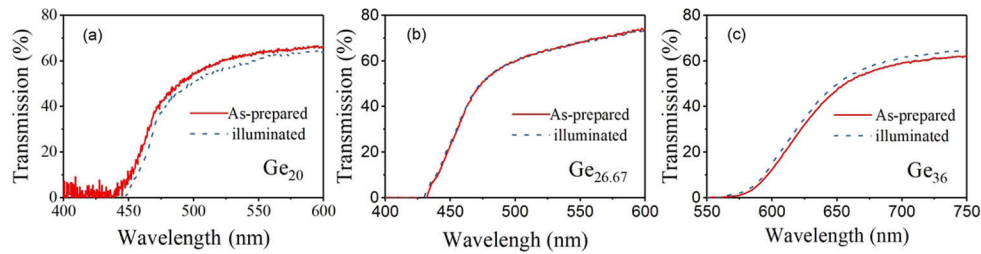


Fig. 2. Transmission spectra of as-prepared (red, solid) and illuminated (10000 s, dash) Ge-Ga-S samples (a) Ge_{20} ($\text{Ge}_{20}\text{Ga}_8\text{S}_{72}$), (b) $\text{Ge}_{26.67}$ ($\text{Ge}_{26.67}\text{Ga}_8\text{S}_{65.33}$), and (c) Ge_{36} ($\text{Ge}_{36}\text{Ga}_8\text{S}_{56}$), respectively.

$\text{Ge}_{26.67}$ and Ge_{36} show different behaviors. There is no visible change in the optical band gap of $\text{Ge}_{26.67}$ before and after illumination, while the optical bandgap energy of Ge_{36} increases from 1.73 eV to 1.76 eV, and this further increases to 1.81 eV upon annealing, indicating an irreversible PB process.

Table 1. The optical bandgap energy of the as-prepared, illuminated (with different power densities) and annealed samples extracted from the Tauc plots.

Sample	State	Optical bandgap energy (eV)(± 0.01 eV)			
		Illumination power density (mW/cm^2)			
		10	122	244	400
$\text{Ge}_{20}\text{Ga}_8\text{S}_{72}$	As-prepared	2.45	2.45	2.45	2.45
	Illuminated	2.4	2.4	2.4	2.42
	Annealed				2.45
$\text{Ge}_{26.67}\text{Ga}_8\text{S}_{65.33}$	As-prepared	2.33	2.33	2.33	2.33
	Illuminated	2.33	2.33	2.33	2.33
	Annealed				2.33
$\text{Ge}_{36}\text{Ga}_8\text{S}_{56}$	As-prepared	1.73	1.73	1.73	1.73
	Illuminated	1.76	1.76	1.76	1.76
	Annealed				1.81

It is well known that, the determination of the bandgap from the Tauc plots could have an error bar of 0.01 eV. The present results regarding the change of the optical bandgap is larger than the error bar, and thus confirming the validity of the present approach. The change of the optical bandgap upon illumination in Table 1 is also in agreement with Fig. 2, where Figs. 2(a) and (c) exhibit observable shift of the transmission edge.

We excluded the possible thermal effect during illumination. Schardt et al. [27] reported that under the irradiation of 800nm laser with a power from 50 to 400 mW/cm^2 , the temperature of the irradiated point was only about 5K. Our previous results using infrared thermal image also showed that the temperature rise of the film irradiated by the 655 nm laser with power of 400 mW/cm^2 is less than 3 K [28]. Such a smaller temperature raise has negligible effect on photo-induced effects in the samples.

We recorded the transmission spectra of the samples in the dark, and expressed it as T_i . Then, we turned on the pump beam and recorded the transmission spectrum as (T_f). Finally, T_f/T_i at a certain wavelength was used to investigate the kinetic process of photo-induced effects in samples. In our case, we took a wavelength where the sample has a transmittance of 30% in the dark in the as-prepared state. Figure 3 show three distinct behaviors. For Ge_{20} , T_f/T_i decreases down

to 0.85 with prolonged illumination time up to 10000s. For the $\text{Ge}_{26.67}$, T_f/T_i ratio is almost unchanged at 1. For the Ge_{36} , when the pump laser is turned on, the real-time transmission decreases initially up to 200 s, and then increases gradually with the prolonged illumination. We can conclude that the photobleaching occurs in Ge_{36} during this process.

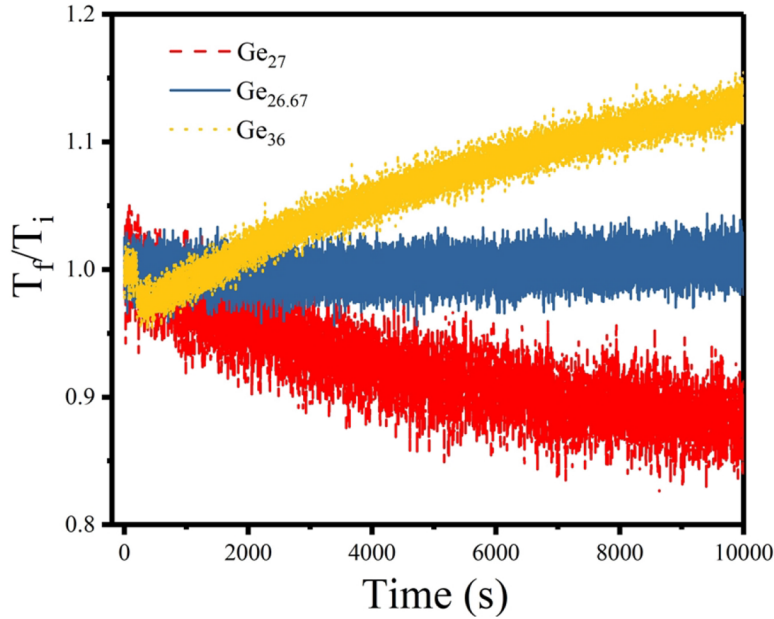


Fig. 3. Time evolution of T_f/T_i for Ge_{20} , $\text{Ge}_{26.67}$, and Ge_{36} samples illuminated by an 830 nm LED with a power intensity of 244 mW/cm^2 .

The whole dynamic process can be regarded as the linear sum of the contributions from both PD and PB processes. In order to simulate the reaction kinetics of photo-induced effects under four different illuminated power densities, we use the combination of stretching exponential functions to describe photo-induced effects [29] with the quality of the fit as R-square=0.97463:

$$\Delta T = A[\exp\{-(t/\tau_d)^{\beta_d}\}] + \Delta T_{sd} + \Delta T_{sb}[1 - \exp\{-(t/\tau_b)^{\beta_b}\}] \quad (1)$$

where the subscript d corresponds to PD. ΔT_{sd} , ΔT_{sb} are the metastable part, τ_d , τ_b are the time constant, β_d , β_b are the dimensionless parameter, t is the illumination time, A is a temperature dependent quantity that is equal to the maximum transient changes. The value between the initial and final process of T_f/T_i , which is determined by the fitting stretched exponential function, is defined as ΔT .

Figures 4(a) and (b) show T_f/T_i vs. illumination time for Ge_{20} and Ge_{36} samples with different illumination power densities, respectively. Each curve in Fig. 3 is fitted by Eq. (1) and all the fitting parameters are listed in Table 2. For Ge_{20} sample, T_f/T_i exhibits a tendency to decrease with prolonged illumination, corresponding to a PD process. Such a decrease can be accelerated with the increase of illumination power density as shown in Fig. 3(a). Such an acceleration process is reflected by both decreasing τ_d and ΔT_{sd} in Table 2. When the illumination power density increases from 10 to 400 mW/cm^2 , τ_d decreases from 10640 s to 2700 s, but ΔT_{sd} decreases from 0.88 to 0.61. On the other hand, T_f/T_i in Ge_{36} shows an initial decrease and then converts to a gradual increase overtaking its initial value of 1. Such mixed PD and PB behavior is similar to that has been found in $\text{Ge}_{19}\text{As}_{21}\text{Se}_{60}$ [29]. In Table 2, both τ_d and τ_b in Ge_{36} gradually increases with decreasing power density, more than one order of magnitude difference in τ_d and τ_b indicates that, PD is a fast response to the illumination while PB is relatively slow.

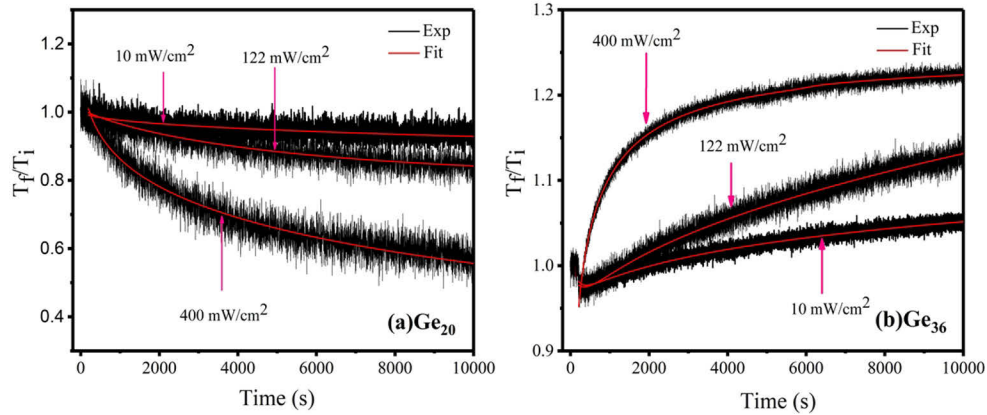


Fig. 4. Time evolution of T_f/T_i at 10, 122 and 400 mW/cm^2 for Ge_{20} (a), and Ge_{36} (b), respectively. The black lines are the experimental results, while the red lines are the fitting based on the Eq. (1).

Table 2. The fitting parameters of photo-induced effects in Ge_{20} and Ge_{36} samples at different power densities

Sample	Power Density (mW/cm^2)	τ_d (s)	β_d	ΔT_{sd}	τ_b (s)	β_b	ΔT_{sb}
$\text{Ge}_{20}\text{Ga}_8\text{S}_{72}$	10	10640	0.64	0.88	0	0	0
	122	5300	0.84	0.80	0	0	0
	244	4800	0.87	0.84	0	0	0
	400	2700	0.88	0.61	0	0	0
$\text{Ge}_{36}\text{Ga}_8\text{S}_{56}$	10	350	0.21	0.51	9300	0.31	0.78
	122	270	0.33	0.53	8600	0.47	0.85
	244	160	0.24	0.55	6300	0.53	0.85
	400	10	0.24	0.54	200	0.34	0.94

Figures 5(a) and (b) show the response of Ge_{20} and Ge_{36} samples to switching-on and -off of the illumination, respectively. Switching-off the illumination causes the increase of T_f/T_i . The initial value of T_f/T_i can be restored by turning on the light again. In all cases, the difference of T_f/T_i between switching-on and -off increases with increasing illumination power. The behavior is similar to that in [25,29,30], where the change of T_f/T_i during on-off cycles was ascribed to the mixture of the transient photodarkening (during the pump period) and metastable PD for Ge_{20} or PB for Ge_{36} (during the rest period). Once the pump beam is switched off, the transmission increases and saturates quickly. When the illumination is switched on, transmission decreases and reaches the values before the illumination is switched off. In subsequent “on/off” series, transient photodarkening is followed by build-up of metastable PD for Ge_{20} or PB for Ge_{36} glass, leading to enhanced amplitude of PD for Ge_{20} in Fig. 5(a) or PB for Ge_{36} in Fig. 5(b) during each next resting cycle. This especially becomes obvious with increasing illumination power density or prolonged illumination duration.

We notice that, while the degree of photo-induced effects is sensitive to light intensity as the data presented above, photon energy of the illumination light more or less than optical bandgap of the glasses could also have different effect on the photo-induced effects [4,18]. Nevertheless, the illumination energy of 1.49 eV (830 nm) used in the paper is close to or less than the band gap energy of the samples in any states (e.g., as-prepared, illuminated, annealed states) as shown

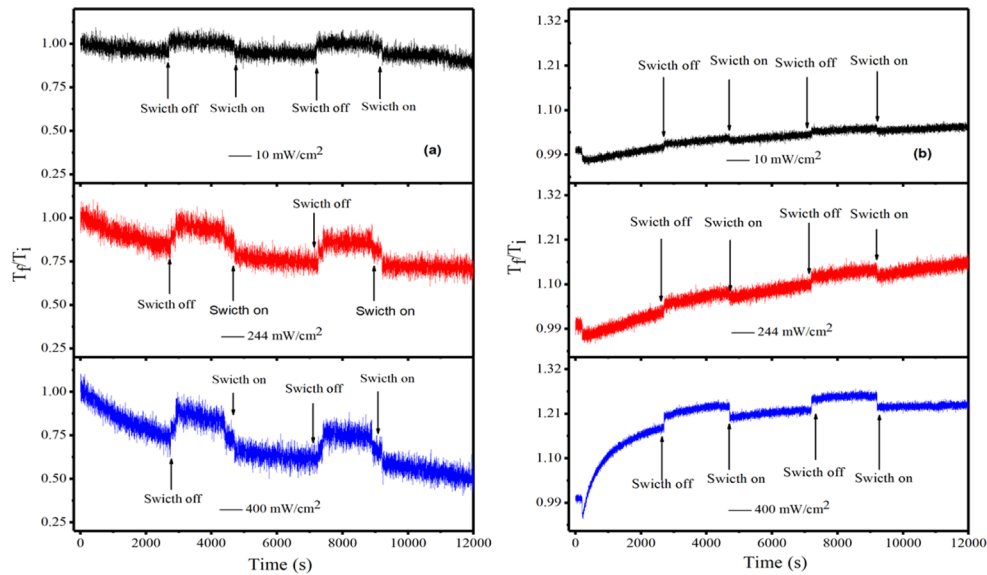


Fig. 5. Photoinduced effects of Ge_{20} (a) and Ge_{36} (b) under different illumination power densities

in Table 1, and this makes it possible to compare all the PIEs induced by the sub-bandgap light in different samples.

Regarding the origin of the photo-induced effects, it has been suggested that the darkening effect is caused by the photoinduced broadening at the top of the valence band, increasing Ge content at the expense of S results in a sulfur deficient network, promoting a conversion of isolated GeS_4 to corner- or edge-sharing GeS_4 tetrahedra units and $\text{Ge}_x\text{S}_{(3-x)}\text{Ge}-\text{GeS}_{(3-x)}\text{Ge}_x$ units, with a corresponding reduction in S–S bonds. The presence of Ge–Ge bonds, which have lower bond energy and higher bond susceptibility than those of S–S bonds, is responsible for the decrease in optical band gap and enhancement of refractive index [25,30,31]. However, we do not observe any structural changes from Raman scattering spectra of the as-prepared and illuminated samples, probably due to the thick bulk samples used in the experiments.

While the origin of the photo-induced effects in chalcogenide glasses is still arguable, our on-going interest is to develop stable host glasses for rare earth ion doping, in which PD should be minimized otherwise the additional optical loss can be introduced. Andriesh et.al. investigated the optical loss and optical-induced absorption in chalcogenide fiber [32]. When extrinsic impurities like hydrides (OH , H_2) oxides and hydro-carbonates impurities, which are one of the important factors to induce optical loss in the materials, can be further reduced with the development of the technologies in the research laboratory, intrinsic photo-induced absorption effect can cause the decrease of the intensity of the probing light at the output of the fibre when illuminating the lateral surface of the fiber with bandgap light. Photo-induced increase in optical loss has also been discovered in waveguide of Ge-Ga-Se [17]. This is a big concern for the active applications like amplifier and lasing, since the signal enhancement from Er^{3+} should exceed the loss of the host glass before the net gain is achieved [14]. We note that, in previous studies, the composition used for chalcogenide waveguide amplifiers are mostly Ge-poor, where the strong PD leads to additional loss and thus reduce the net optical gain in the waveguide.

The present results present clear evidence that, chemically stoichiometric $\text{Ge}_{26.67}\text{Ga}_8\text{S}_{65.33}$ samples exhibit the minimum photo-induced effect in the continuous illumination process, where T_f/T_i has no observable change with the increase of laser power density. Therefore, it could

be the best choice of glass composition for waveguide manufacturing in applications of optical amplifiers. This is understandable based on the conversion of heteropolar to homopolar bonds induced by PD [4,18]. The formation of the homopolar bonds increases the number of the wrong bonds in the glasses and thus increases the optical loss. Therefore, a significant approach could be reducing the intrinsic losses caused by PD via compositional design, which is obviously viable from the present results. Further investigation on the correlation between PB and optical loss may offer an interesting opportunity to see whether strong PB effect could further reduce the optical losses and thus increase the gain of the waveguide using Ge-rich Ge-Ga-S glasses.

4. Conclusion

We have prepared Ge-Ga-S glasses with different compositions, and studied the photo-induced effects in the as-prepared, illuminated and annealed states of the samples. We found that, while PD and PB appear in the Ge-poor and Ge-rich samples, the chemically stoichiometric Ge_{26.67} sample show no visible photo-induced effects. The dependence T_f / T_i on illumination time and power density indicates that, PD and PB increases with increasing illumination time and power density in Ge₂₀ and Ge₃₆ samples, respectively. While PD behavior certainly has negative effect on the optical loss of the glass, the present results demonstrate that, the chemically stoichiometric Ge_{26.67} sample could be the best choice as host glasses for rare earth ion doping in waveguide-based amplifier since additional optical loss induced by PD can be suppressed. Nevertheless, it is also possible to use PB effects decreasing optical loss of the materials if further investigation can confirm the positive correlation between the PB and optical loss.

Funding. Key Technologies Research and Development Program (2020YFB1805900); National Natural Science Foundation of China (61775109); 3315 Innovation Team in Ningbo City.

Acknowledgements. This work is supported by the National Key R&D Program of China (2020YFB1805900); National Science Foundation of China (Grant No. 61775109); 3315 Innovation Team in Ningbo City, Zhejiang Province, China.

Disclosures. The authors declare no conflicts of interest.

Data availability. Data underlying the results presented in this paper are not publicly available at this time but may be obtained from the authors upon reasonable request.

References

1. B. J. Eggleton, B. Luther-Davies, and K. Richardson, "Chalcogenide photonics," *Nat. Photonics* **5**(3), 141–148 (2011).
2. A. Zakery and S. R. Elliott, "Optical properties and applications of chalcogenide glasses: a review," *J. Non-Cryst. Solids* **330**(1-3), 1–12 (2003).
3. R. P. Wang, *Amorphous Chalcogenides: Advances and Applications* (Pan Stanford Publishing, 2014).
4. K. Tanaka and K. Shimakawa, *Amorphous Chalcogenide Semiconductors and Related Materials* (Springer, 2011).
5. Yu. S. Tveryanovich and A. Tveranovich, *Rare-Earth Doped Chalcogenide Glasses in Semiconducting Chalcogenide Glasses III* (Academic Press, 2004).
6. A. B. Seddon, Z. Tang, D. Furniss, S. Sujecki, and T. M. Benson, "Progress in rare-earth-doped mid-infrared fiber lasers," *Opt. Express* **18**(25), 26704–26719 (2010).
7. S. D. Jackson, "Towards high-power mid-infrared emission from a fiber laser," *Nat. Photonics* **6**(7), 423–431 (2012).
8. T. H. Lee, S. I. Simdyankin, J. Hegedus, J. Heo, and S. R. Elliott, "Spatial distribution of rare-earth ions and tetrahedra in chalcogenide glasses studied via laser spectroscopy and ab initio molecular dynamics simulation," *Phys. Rev. B* **81**(10), 104204 (2010).
9. R. Wang, K. Yan, M. Zhang, X. Shen, S. Dai, X. Yang, Z. Yang, A. Yang, B. Zhang, and B. Luther-Davies, "Chemical environment of rare earth ions in Ge_{28.125}Ga_{6.25}S_{65.625} glass-ceramics doped with Dy³⁺," *Appl. Phys. Lett.* **107**(16), 161901 (2015).
10. T. Schweizer, D. W. Hewak, D. N. Payne, T. Jensen, and G. Huber, "Rare earth doped chalcogenide glass laser," *Electron. Lett.* **32**(7), 666–667 (1996).
11. T. Schweizer, B. N. Samson, R. C. Moore, D. W. Hewak, and D. N. Payne, "Rare-earth doped chalcogenide glass fibre laser," *Electron. Lett.* **33**(5), 414 (1997).
12. H. Tawarayama, E. Ishikawa, K. Yamanaka, K. Itoh, K. Okada, H. Aoki, H. Yanagita, Y. Matsuoka, and H. Toratani, "Optical amplification at 1.3 μ m in a praseodymium-doped sulfide-glass fiber," *J. Am. Ceram. Soc.* **83**(4), 792–796 (2004).

13. A. K. Mairaj, C. Riziotis, A. M. Chardon, P. G. R. Smith, D. P. Shepherd, and D. W. Hewak, "Development of channel waveguide lasers in Nd³⁺-doped chalcogenide (Ga: La: S) glass through photoinduced material modification," *Appl. Phys. Lett.* **81**(20), 3708–3710 (2002).
14. K. Yan, K. Vu, and S. Madden, "Internal gain in Er-doped As₂S₃ chalcogenide planar waveguides," *Opt. Lett.* **40**(5), 796 (2015).
15. M. F. Churbanov, M. V. Sukhanov, and A. P. Velmuzhov, "First demonstration of ~ 5 μm laser action in terbium-doped selenide glass," *Appl. Phys. B* **126**(7), 117 (2020).
16. M. F. Churbanov, G. E. Snopatin, and M. V. Sukhanov, "Laser potential of Pr³⁺ doped chalcogenide glass in 5-6 μm spectral range," *J. Non-Cryst. Solids* **559**, 120592 (2021).
17. Kunlun Yan, "Rare-earth doped chalcogenide waveguide amplifiers," PhD. Thesis, Australian National University, 2016.
18. M. Frumar, B. Frumarova, T. Wagner, and P. Nemeč, "Photo-induced phenomena in amorphous and glassy chalcogenides," in A. V. Kolobov (Ed.), *Photo-induced Metastability in Amorphous Semiconductors* (Wiley-VCH, 2003), pp. 27–28.
19. Q. Yan, H. Jain, J. Ren, D. Zhao, and G. Chen, "Effect of photo-oxidation on photobleaching of GeSe₂ and Ge₂Se₃ films," *J. Phys. Chem. C* **115**(43), 21390–21395 (2011).
20. Y. Liu, H. Jain, J. Ren, Q. Yan, and G. Chen, "High-resolution X-ray photoelectron spectroscopy study of photo-oxidation of amorphous oxy chalcogenide films," *J. Phys. Chem. C* **116**(46), 24590–24595 (2012).
21. C. Laurent, Y. Zhiyong, and L. Pierre, "light-induced matrix softening of Ge-As-Se network glasses," *Phys. Rev. Lett.* **101**(17), 177402 (2008).
22. G. Yang, H. Jain, A. Ganjoo, D. Zhao, Y. Xu, H. Zeng, and G. Chen, "A photo-stable chalcogenide glass," *Opt. Express* **16**(14), 10565 (2008).
23. X. Q. Su, R. P. Wang, and B. Luther-Davies, "The dependence of photosensitivity on composition for thin films of Ge_xAs_ySe_{1-x-y} chalcogenide glasses," *Appl. Phys. A* **113**, 575–581 (2013).
24. P. Němec, S. Zhang, V. Nazabal, K. Fedus, and X. H. Zhang, "Photo-stability of pulsed laser deposited Ge_xAs_ySe_{100-x-y} amorphous thin films," *Opt. Express* **18**(22), 22944–22957 (2010).
25. P. Khan, H. Jain, and K. V. Adarsh, "Role of Ge:As ratio in controlling the light-induced response of a-Ge_xAs_{35-2x}Se₆₅ thin films," *Sci. Rep.* **4**(1), 4029 (2015).
26. X. Yang, M. Zhang, K. Yan, L. Han, Q. Xu, H. Liu, and R. Wang, "Controllable formation of the crystalline phases in Ge-Ga-S chalcogenide glass-ceramics," *J. Am. Ceram. Soc.* **100**(1), 74–80 (2017).
27. C. R. Schardt, P. Lucas, A. Doraiswamy, P. Jivaganont, and J. H. Simmons, "Raman temperature measurement during photostructural changes in Ge_xSe_{1-x} glass," *J. Non-Cryst. Solids* **351**(19-20), 1653–1657 (2005).
28. S. Zhang, Y. Chen, R. Wang, X. Shen, and S. Dai, "Observation of photobleaching in Ge-deficient Ge_{16.8}Se_{83.2} chalcogenide thin film with prolonged irradiation," *Sci. Rep.* **7**(1), 14585 (2017).
29. P. Khan, A. R. Barik, E. M. Vinod, K. S. Sangunni, H. Jain, and K. V. Adarsh, "Coexistence of fast photodarkening and slow photobleaching in Ge₁₉As₂₁Se₆₀ thin films," *Opt. Express* **20**(11), 12416–12421 (2012).
30. A. Mishchenko, J. Berashevich, K. Wolf, D. A. Tenne, A. Reznik, and M. Mitkova, "Dynamic variations of the light-induced effects in a-Ge_xSe_{100-x} films: experiment and simulation," *Opt. Mater. Express* **5**(2), 295–306 (2015).
31. V. Lyubin, M. Klebanov, A. Burner, N. Shitrit, and B. Sfez, "Transient photodarkening and photobleaching in glassy GeSe₂ films," *Opt. Mater.* **33**(6), 949–952 (2011).
32. A. M. Andriesh, I. P. Culeac, and V. M. Loghin, "Photoinduced changes of optical absorption in chalcogenide glass fibers," *Pure Appl. Opt.* **1**(2), 91–102 (1992).